university of groningen

University Medical Center Groningen

University of Groningen

Three-way stabilization of the covalent intermediate in amylomaltase, an alpha-amylase-like transglycosylase

Barends, Thomas R. M.; Bultema, Jelle B.; Kaper, Thijs; van der Maarel, Marc J. E. C.; Dijkhuizen, Lubbert; Dijkstra, Bauke W.

Published in:
The Journal of Biological Chemistry

DOI:
10.1074/jbc.M701444200

IMPORTANT NOTE: You are advised to consult the publisher's version (publisher's PDF) if you wish to cite from it. Please check the document version below.

Document Version
Publisher's PDF, also known as Version of record

Publication date:
2007

Link to publication in University of Groningen/UMCG research database

Citation for published version (APA):
Barends, T. R. M., Bultema, J. B., Kaper, T., van der Maarel, M. J. E. C., Dijkhuizen, L., & Dijkstra, B. W. (2007). Three-way stabilization of the covalent intermediate in amylomaltase, an alpha-amylase-like transglycosylase. *The Journal of Biological Chemistry*, *282*(23), 17242-17249. https://doi.org/10.1074/jbc.M701444200

Copyright
Other than for strictly personal use, it is not permitted to download or to forward/distribute the text or part of it without the consent of the author(s) and/or copyright holder(s), unless the work is under an open content license (like Creative Commons).

The publication may also be distributed here under the terms of Article 25fa of the Dutch Copyright Act, indicated by the “Taverne” license. More information can be found on the University of Groningen website: https://www.rug.nl/library/open-access/self-archiving-pure/taverne-amendment.

Take-down policy
If you believe that this document breaches copyright please contact us providing details, and we will remove access to the work immediately and investigate your claim.

Downloaded from the University of Groningen/UMCG research database (Pure): http://www.rug.nl/research/portal. For technical reasons the number of authors shown on this cover page is limited to 10 maximum.

THE JOURNAL OF BIOLOGICAL CHEMISTRY VOL. 282, NO. 23, pp. 17242–17249, June 8, 2007
© 2007 by The American Society for Biochemistry and Molecular Biology, Inc. Printed in the U.S.A.

Three-way Stabilization of the Covalent Intermediate in Amylomaltase, an α-Amylase-like Transglycosylase*

Received for publication, February 19, 2007, and in revised form, March 27, 2007 Published, JBC Papers in Press, April 9, 2007, DOI 10.1074/jbc.M701444200

Thomas R. M. Barends[‡§1], Jelle B. Bultema[‡], Thijs Kaper[§¶], Marc J. E. C. van der Maarel[§¶], Lubbert Dijkhuizen[§¶], and Bauke W. Dijkstra[‡§2]

From the [‡]Laboratory of Biophysical Chemistry, University of Groningen, Nijenborgh 4, 9747 AG Groningen, [§]Centre for Carbohydrate Bioprocessing, TNO-University of Groningen, Kerklaan 30, 9751 Haren, and [¶]Laboratory of Microbiology, University of Groningen, Kerklaan 30, 9751 Haren, The Netherlands

Amylomaltases are glycosyl hydrolases belonging to glycoside hydrolase family 77 that are capable of the synthesis of large cyclic glucans and the disproportionation of oligosaccharides. Using protein crystallography, we have generated a flip book movie of the amylomaltase catalytic cycle in atomic detail. The structures include a covalent glycosyl enzyme intermediate and a covalent intermediate in complex with an analogue of a co-substrate and show how the structures of both enzyme and substrate respond to the changes required by the catalytic cycle as it proceeds. Notably, the catalytic nucleophile changes conformation dramatically during the reaction. Also, Gln-256 on the 250s loop is involved in orienting the substrate in the +1 site. The absence of a suitable base in the covalent intermediate structure explains the low hydrolysis activity.

Amylomaltases are 4-α-glucanotransferase enzymes (1–4) that are structurally and mechanistically related to α-amylases (family 13 of the glycoside hydrolases or GH13) (5–7) despite their classification in a separate glycoside hydrolase family (glycoside hydrolase family 77). However, amylomaltases almost exclusively catalyze transglycosylation reactions, whereas α-amylase-like enzymes mostly catalyze hydrolysis. As a result, the amylomaltases perform so-called disproportionation reactions, the net effect of which is that two amylose chains of certain lengths react in such a way that one of the chains (the "donor") becomes shorter and the other one (the "acceptor") longer as shown in Reaction 1.

$$G_x + G_y \xrightarrow{\text{amylomaltase}} G_{x+n} + G_{y-n}$$

REACTION 1

Instead of using two different sugar chains for this reaction, the enzyme can also take the non-reducing end of the donor substrate as the acceptor substrate, which results in the formation of a cyclic glucan product of at least 16 glucose units (8–11). These properties, amylose disproportionation and the synthesis of large cyclic glucans, make these enzymes interesting biocatalysts for the synthesis of valuable fine chemicals and pharmaceutically important materials (12–14).

Over the years, several incisive studies have contributed to our current understanding of catalysis by α-amylase-type enzymes. Importantly, a structure of a covalent reaction intermediate, obtained by Uitdehaag *et al.* (15), provided a detailed look into the active site, showing among other things how the (mutated) acid/base catalyst is poised to activate a water molecule for attack on the C_1 carbon atom. Since then, two other examples of covalent glycosyl enzyme intermediate structures of α-amylase-type enzymes have been published (16, 17). These structures provided insight into the hydrolysis mechanism, *i.e.* in the way in which a covalent intermediate is attacked by a water molecule. Three conserved carboxylic acid residues play a central role in the catalytic mechanism (15, 18–20). The first carboxylic acid residue acts as an acid/base catalyst that protonates the oxygen atom of the scissile glycosidic bond. Simultaneously, the C_1 carbon atom is attacked by the second carboxylate, the nucleophile, which results in the formation of a covalent glycosyl enzyme intermediate through a planar, oxocarbenium ion-like transition state. This covalent intermediate can be broken down through nucleophilic attack on the C_1 carbon atom of the sugar, either by a water molecule, resulting in hydrolysis, or by a hydroxyl group of another sugar molecule, the glycosyl acceptor, resulting in the formation of a new glycosidic bond. The third carboxylate binds the sugar in the −1 subsite (for nomenclature of sugar binding subsites see Ref. (21)), distorting it toward a partially planar conformation in the Michaelis complex and contributing to the stabilization of the transition state, all through hydrogen bonds to the 2- and 3-hydroxyl groups. However, so far no direct evidence has been obtained for how the covalent intermediate is attacked by another sugar, but amylomaltases seem ideal for studying this, given their low hydrolysis activity.

The first amylomaltase structures to become available were of the enzyme from *Thermus aquaticus*, both uncomplexed and in a complex with two molecules of the pseudo-tetrasaccharide inhibitor acarbose (11, 22, 23). The structures showed the expected $(\beta/\alpha)_8$-barrel fold and active site build-up of an α-am-

* This work was supported by European Union 5FP CEGLYC Project (Contract QLK3-CT-2001-00149). The costs of publication of this article were defrayed in part by the payment of page charges. This article must therefore be hereby marked "*advertisement*" in accordance with 18 U.S.C. Section 1734 solely to indicate this fact.

The atomic coordinates and structure factors (code 2OWW, 2OWC, and 2OWX) have been deposited in the Protein Data Bank, Research Collaboratory for Structural Bioinformatics, Rutgers University, New Brunswick, NJ (http://www.rcsb.org/).

[1] Present address: Max Planck Institute for Medical Research, Jahnstrasse 29, D-69120 Heidelberg, Germany.

[2] To whom correspondence should be addressed. Fax: 31-50-3634800; E-mail: b.w.dijkstra@rug.nl.

Downloaded from www.jbc.org at University of Groningen on June 28, 2007

TABLE 1
Data collection and refinement statistics

	Native, pH 5.6, PDB code 2OWX	Covalent intermediate with acarbose, PDB code 2OWC	Covalent intermediate: 4-deoxyglucose complex, PDB code 2OWW
X-ray source	BW7A (EMBL, Hamburg)	ID14-1 (ESRF, Grenoble)	FR591 rotating anode
Space group, unit cell	$P3_121$, $a = b = 93.8$, $c = 154.8$ Å	$P3_121$, $a = b = 92.4$, $c = 154.1$ Å	$P3_121$, $a = b = 92.5$, $c = 154.2$ Å
Resolution range	99–2.50 Å	30–1.90 Å	30–2.20 Å
Completeness	90.9%[a]	100%	98.5%
R_{merge}[b]	0.094 (0.52)	0.084 (0.79)[c]	0.13 (0.59)
$I/\theta(I)$[b]	10.1 (1.8)	24 (2.4)	15 (4.5)
Resolution range in refinement	99–2.50 Å	30–2.05 Å[c]	30–2.20 Å
Highest resolution shell in refinement	2.53–2.50 Å	2.10–2.05 Å	2.26–2.20 Å
Number of reflections in refinement	23787	46013	36721
(Highest resolution shell)	1858	3354	2618
Number of atoms in refinement	4176	4545	4496
No. of ligand molecules in asymmetric unit			
Covalently bound acarbose	0	1	1
4-Deoxyglucose	0	0	1
Glycerol	1	0	2
Malonate	1	1	1
Water	103	411	322
***R*-factor (highest resolution)**	0.220 (0.305)	0.186 (0.209)	0.198 (0.262)
R_{free} (highest resolution)	0.276 (0.356)	0.216 (0.253)	0.240 (0.312)
Average B factor (Å^2) all atoms	45.45	27.62	29.14
Covalent intermediate alone	n.a.[d]	23.29	34.50
4-Deoxyglucose alone	n.a.[d]	n.a.[d]	58.31
Root mean square deviation from geometry target values			
Bond lengths (Å^2)	0.008	0.008	0.008
Angles (°)	1.4	1.1	1.1
% age of residues in region of Ramachandran plot			
Allowed	91.8	93.0	91.3
Additional allowed	8.2	7.0	8.7
Generously allowed	0.0	0.0	0.0
Disallowed	0.0	0.0	0.0

[a] The completeness of this data set is limited to 90% due to ice rings.
[b] Values in parentheses denote the R_{merge} and $\langle I\rangle/\langle\theta(I)\rangle$ in the highest resolution shell.
[c] Because of the high R_{merge} in the highest resolution shell, the data used for refinement were limited to 2.05 Å where the $R_{merge} = 0.42$ and $I/s(I) = 5.0$.
[d] n.a., not applicable.

ylase-type enzyme. However, in the acarbose complex two of the catalytic residues, the catalytic nucleophile Asp-293 and the acid/base catalyst Glu-340, were found to point away from the site of cleavage of the glycosidic bond of the substrate, *i.e.* to have incompetent orientations for catalysis. This was tentatively attributed to the high pH of the soaking experiment (pH 9.0), which was deemed necessary to avoid enzymatic hydrolysis of the inhibitor (22). The third carboxylate, the transition state stabilizer Asp-395, did bind the 2- and 3-OH groups of the inhibitor in the −1 subsite as expected.

Here we report the structure of the amylomaltase from *Thermus thermophilus* close to the optimum pH, along with a covalent reaction intermediate obtained in a native active site (*i.e.* without any mutations), also close to the optimum pH, as well as a complex of this covalent intermediate with the acceptor analogue 4-deoxyglucose. Because the *Th. thermophilus* and *Th. aquaticus* enzymes differ only in one amino acid, on a surface site remote from the active site (glutamine 27 in the *Th. thermophilus* enzyme is an arginine in the *Th. aquaticus* protein), our results can be readily combined with the acarbose complex structure reported previously by Przylas *et al.* (22, 23), yielding a step-by-step flip book movie of the entire catalytic cycle in atomic detail, including the attack of the incoming acceptor substrate on the covalent intermediate. The new structures show the reasons for the low hydrolysis activity as well as the binding mode of an acceptor of the glycosyl moiety. Overall, these new structures reveal how the enzyme protects the covalent intermediate from attack by an undesired nucleophile.

MATERIALS AND METHODS

Protein Preparation—His-tagged *Th. thermophilus* amylomaltase was purified by heat incubation and nickel-nitrilotriacetic acid affinity chromatography from *Escherichia coli* BL21(DE-3) cells containing the pCCBmalq plasmid as described elsewhere (24). The protein was concentrated by ultrafiltration to an $A_{280}^{1\ cm}$ of 22 corresponding to ~10 mg/ml and stored at 4 °C.

Crystal Preparation—Removal of the polyhistidine tag proved vital in obtaining high quality amylomaltase crystals. To cleave off the polyhistidine tag, 20 units of bovine thrombin (ICN) dissolved in phosphate-buffered saline (137 mM NaCl, 2.7 mM KCl, 1.4 mM NaH_2PO_4, 4.3 mM Na_2HPO_4, pH adjusted to 7.4 with HCl) with 4 mM β-mercaptoethanol and 4 mM cal-

Downloaded from www.jbc.org at University of Groningen on June 28, 2007

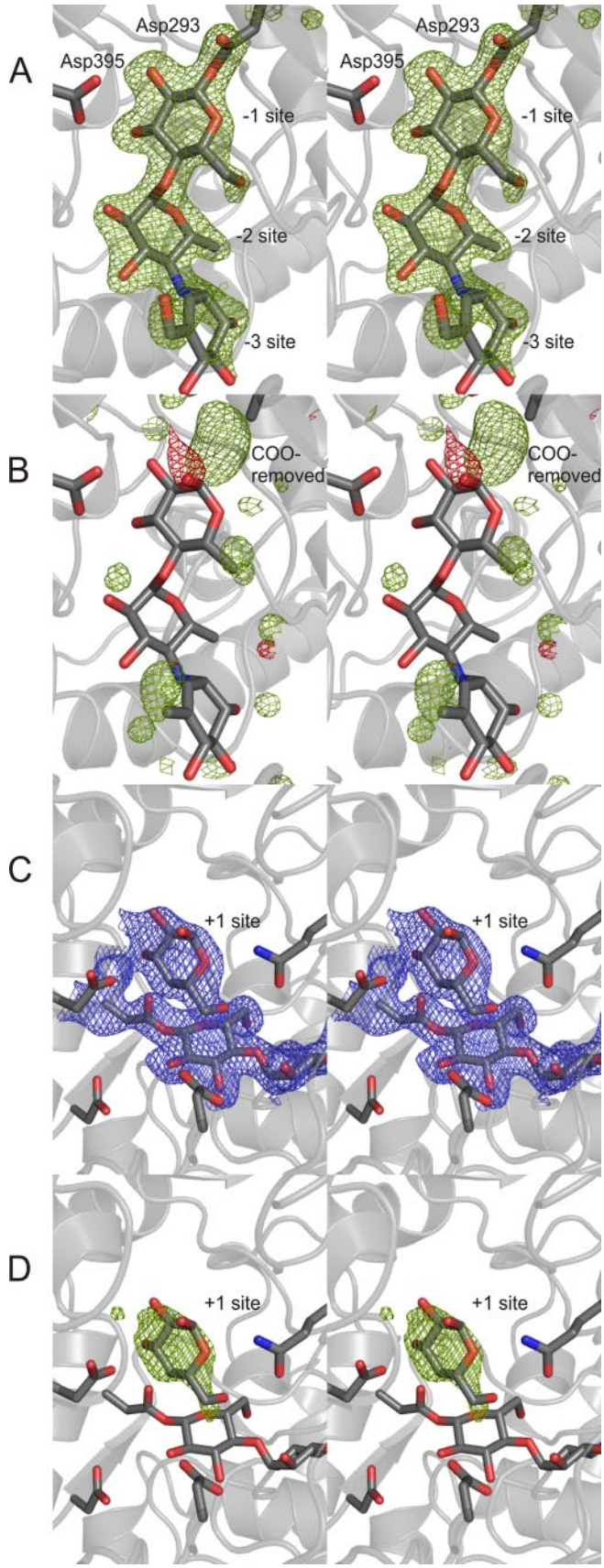

FIGURE 1. **Crystallographic analysis of amylomaltase complexes.** *A*, stereo figure of the $F_o - DF_c$ electron density for acarbose bound to Asp-293, calculated prior to incorporation of acarbose in the model. The density was contoured at 2.5 σ and overlaid on the refined structure. *B*, $F_o - DF_c$ electron density after refinement with a non-covalently bound acarbose. To check the density for the covalent bond and to correctly identify the various acarbose residues, the Asp-293 carboxylate group as well as the acarbose 6-OH groups were omitted from the calculations (see "Materials and Methods"). Positive difference density is shown in *green* (3.5 σ), negative density in *red* (−3.5 σ). $2mF_o - DF_c$ density (*blue*, 1.0 σ) (*C*) $F_o - DF_c$ electron density (*green*, 2.5 σ) (*D*) for the covalent intermediate-4-deoxyglucose complex. To avoid model bias, both maps were calculated prior to the incorporation of 4-deoxyglucose in the model. All figures were produced using PyMol (37).

cium chloride were added to 100 μl of 10 mg/ml His-tagged amylomaltase in 10 mM HEPES/NaOH, pH 7.5 or phosphate-buffered saline, and the reaction was allowed to proceed at room temperature for 24 h. Subsequently, thrombin was inactivated by incubation for 10 min in a water bath at 75 °C, which was followed by centrifugation in an Eppendorf centrifuge at maximum speed for 30 min at 4 °C and dialysis against 10 mM MES[3]/NaOH, pH 6.5, with 1 mM dithiothreitol.

After His tag removal, crystals were grown using the hanging drop vapor diffusion technique in which a drop consisting of 3 μl of the protein solution and 1–3 μl of reservoir solution (0.4–0.8 M sodium malonate (25), pH 5.6, containing 1 mM dithiothreitol) was equilibrated against reservoir solution at room temperature. Rod-shaped crystals grew in 1 week to maximal dimensions of 1.0 × 0.35 × 0.35 mm^3 and were flash-cooled after soaking them briefly in reservoir solution containing 25% glycerol. To obtain a complex with acarbose, a crystal was soaked for 30 min in 500 μl of 0.8 M sodium malonate, pH 5.6, containing 5 mg/ml acarbose (Serva electrophoresis, Heidelberg, Germany) and then flash-cooled in the soaking solution containing 25% glycerol. A complex with acarbose and 4-deoxyglucose was obtained by soaking a crystal for 30 min in 0.8 M sodium malonate, pH 5.6, containing 5 mg/ml acarbose and 120 mg/ml 4-deoxyglucose (CMS Chemicals Ltd., Abingdon, UK), followed by cryoprotection in the same solution with 26% glycerol and flash-cooling in liquid nitrogen.

Data from a native crystal were recorded at the BW7B beam line of the European Molecular Biology Laboratory outstation at the German Synchrotron Research Center in Hamburg, Germany. Data from the acarbose-soaked crystal were collected at the ID14–1 beam line of the European Synchrotron Radiation Facility in Grenoble, France. Data for the acarbose/4-deoxyglucose complex were obtained using CuK-α radiation from a Nonius FR591 rotating anode generator with Osmic mirrors, equipped with a MacScience DIP2030 image plate detector. All data were processed using DENZO and Scalepack (26). Further calculations were performed with software from the CCP4 package (27) unless specified otherwise. Data collection parameters are reported in Table 1.

Structure Solution: Native Structure at pH 5.6—The native structure at pH 5.6 was solved by molecular replacement with the program MolRep (28), using the native *Th. aquaticus* amylomaltase structure of Przylas *et al.* (23) (Protein Data Bank (PDB) code 1CWY) as a starting model, followed by refinement with Refmac5 (29). A comparison was made with the structure published by Przylas *et al.* (23) using the program DynDom version 1.5 (30).

[3] The abbreviations used are: MES, 4-morpholineethanesulfonic acid; PDB, Protein Data Bank.

Downloaded from www.jbc.org at University of Groningen on June 28, 2007

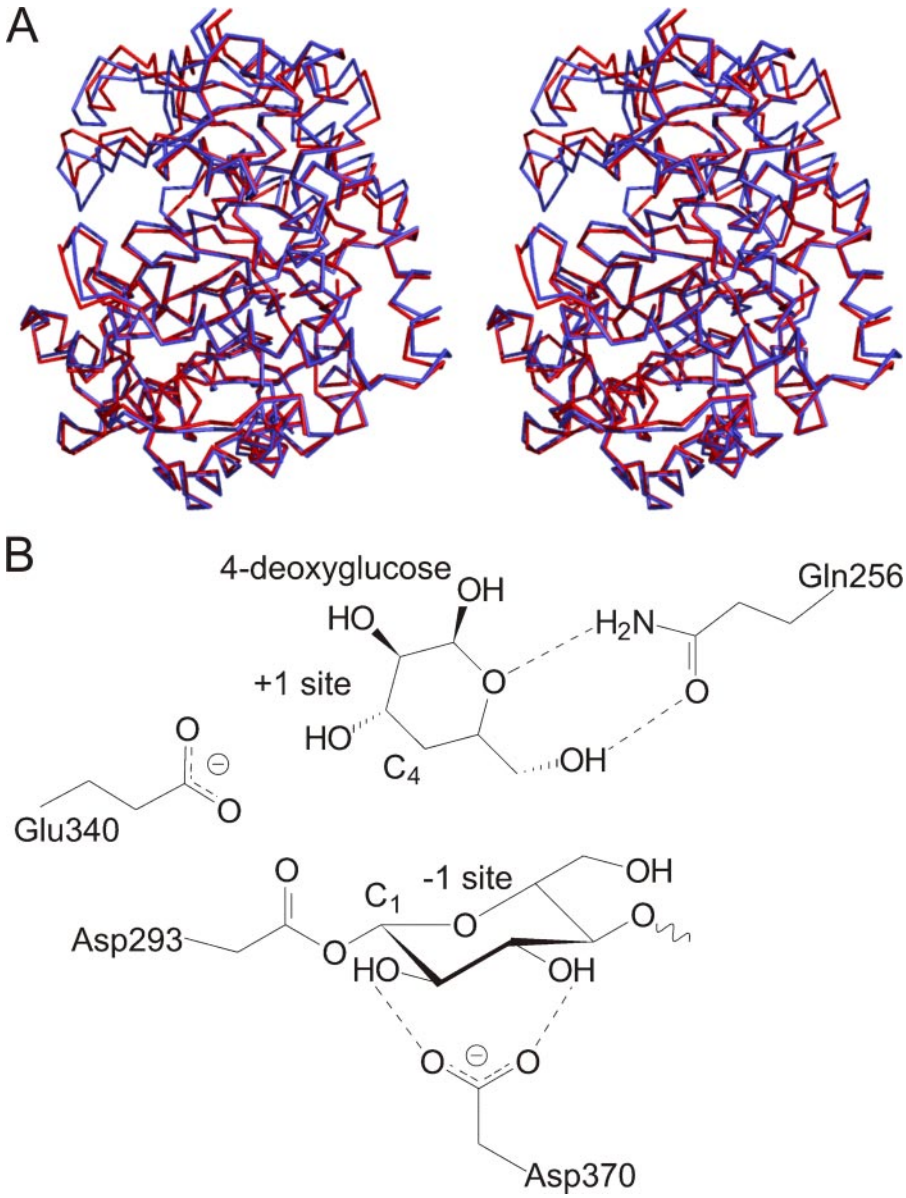

FIGURE 2. *A*, superimposition of the Cα traces of the amylomaltase structure determined by Przylas *et al.* (22) (*red*) and the native structure presented here (*blue*). The superimposition was performed with DynDom (30) (see "Materials and Methods"). *B*, schematic representation of the interactions in the −1 and +1 subsites.

Covalent Intermediate Structure—A difference Fourier electron density map was calculated after brief refinement of the native structure at pH 5.6 against the data for the acarbose-soaked crystal. This showed clear difference electron density for sugar residues in the −1, −2, and −3 sites, with the residue in the −1 site covalently bound to Asp-293 (Fig. 1*A*). To build as unbiased a model as possible, for the next round of refinement three residues of acarbose of which the 6-OH groups had been removed were placed in the density. The carboxylate moiety of Asp-293 was also removed, but the O_1 atom of the sugar residue in the −1 site was kept in its axial position. Difference Fourier maps calculated after refinement of this incomplete structure showed unambiguous difference density for the covalent bond between the −1 sugar residue and the side chain of Asp-293 (Fig. 1*B*), as well as negative difference density for the axial O_1, and allowed identification of the various acarbose residues by the presence or absence of density for a 6-OH group. The model could then be completed and refined using Refmac5 (29).

Covalent Intermediate/4-Deoxyglucose Complex—The covalent intermediate model was briefly refined using Refmac5 against a dataset recorded from a crystal soaked in acarbose and 4-deoxyglucose, and double difference and difference electron density maps showed the presence of a sugar residue in the +1 site (Fig. 1, *C* and *D*). The structure of the complex could then be built and refined using Refmac5 (29) and Xfit (31).

Throughout the refinement of all models, care was taken to use the same set of reflections for the calculation of the free *R*-factor in each case. Refinement statistics are reported in Table 1. Refined structures and diffraction data were deposited in the PDB under accession codes 2OWW, 2OWC and 2OWX.

RESULTS

Crystals of *Th. thermophilus* amylomaltase were obtained at pH 5.6 in a different crystal form from those reported by Przylas *et al.* (22) (space group $P3_121$ with $a = b = 93$ Å, $c = 154$ Å instead of $P6_4$ with $a = b = 154$ Å, $c = 64$ Å). The pH 5.6 structure of the *Th. thermophilus* amylomaltase presented here is very similar to the structures of the *Th. aquaticus* enzyme reported by Przylas *et al.* (22), with root mean square differences of 0.8 Å for the 498 equivalent Cα positions.

However, in the pH 5.6 structure the protein adopts a more closed conformation (Fig. 2*A*). This difference, which is seen when comparing any of the structures presented here with the structures of Przylas *et al.* (22, 23), can be described as being caused by a hinge-like movement around an axis running close to the catalytic nucleophile, Asp-293, mostly affecting the position of the "250s loop" (residues 247–255, see Refs. (11, 22, 23)). Although the electron density for this loop is poor in the pH 5.6 structure, it is clear that because of the rearrangements in the 250s loop a sugar chain in the acceptor subsites would not be able to continue beyond the +2 site. These considerations apply to all new structures reported here. A comparison of the *Th. aquaticus* enzyme with other crystal forms of the *Th. thermophilus* amylomal-

Downloaded from www.jbc.org at University of Groningen on June 28, 2007

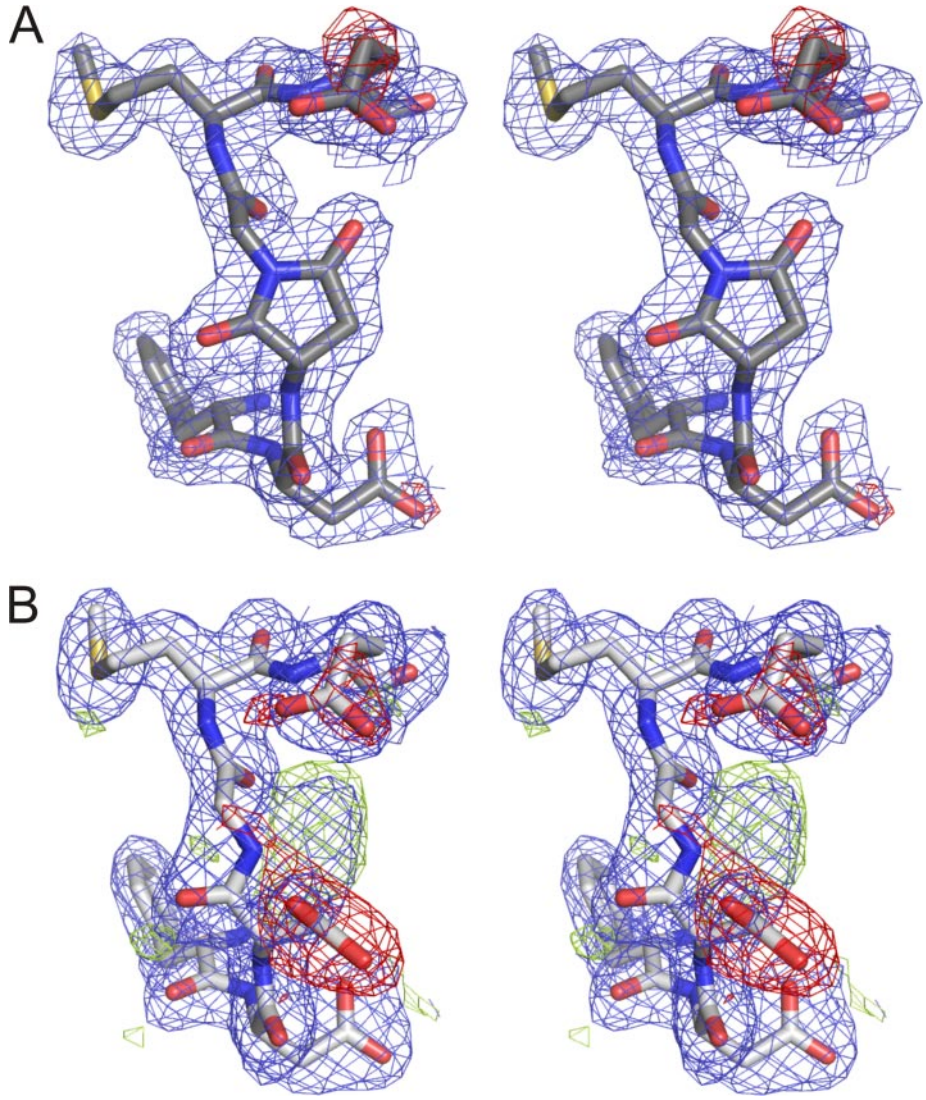

FIGURE 3. **Stereo pictures of the *N*-succinimide in amylomaltase.** *A*, structure of the covalent intermediate model around Asp-370. *B*, the same region in the acarbose complex (PDB code 1ESW) (22). The refined $2mF_o - DF_c$ (*blue*, 1σ) and $F_o - DF_c$ (*green*, 3σ, and *red*, −3σ) densities are overlaid.

tase[4] also showed that the core of the enzyme is rigid, whereas the surface loops are flexible.

N-Succinimide Residue at Position 370–371—In every structure reported here, the residue at position 370, which was expected to be an aspartate, could not be satisfactorily modeled as such. $2mF_o - DF_c$ and $F_o - DF_c$ electron density maps (32) showed that the side chain of Asp-370 had reacted with the main chain amine of Gly-371 to form a succinimide, which was included in the model as such (Fig. 3*A*). Calculation of the electron density for the amylomaltase-acarbose complex structure of Przylas *et al.* (22, 23) using the deposited structure factors show that in that case, too, a succinimide was formed from these residues (Fig. 3*B*) although this was, at the time, not modeled in the deposited structure. Such cyclic amides occur in protein backbones as intermediates in the deamidation of asparagines and in the chemical hydrolysis and rearrangement of the polypeptide chain at Asp/Asn residues. This relatively unusual form of post-translational modification has been observed before in crystal structures, *e.g.* in lysozyme (33). Possibly, the formation of the observed cyclic amide in amylomaltase is accelerated by the high temperature step in the purification and may confer extra stability at the high temperatures at which *Thermus* amylomaltase is active *in vivo*.

Complex Structures—Soaking a *Th. thermophilus* amylomaltase crystal in acarbose resulted in a covalent intermediate bound to Asp-293 consisting of three sugar residues in the −1, −2, and −3 sites (Fig. 1, *A* and *B*). The plane of the ester moiety connecting Asp-293 and the C_1 carbon atom of the −1 sugar is approximately perpendicular to the approximate plane of the −1 sugar ring, in contrast with the situation in the covalent intermediate of CGTase (15) where the two planes are nearly parallel. The catalytic acid/base Glu-340 is oriented away from the active site just as in the native structure at pH 5.6 and the acarbose structure of Przylas *et al.* (22) for *Th. aquaticus* amylomaltase. As expected, the third conserved acidic residue of the α-amylase family, Asp-395, forms hydrogen bonds with the 2-OH and 3-OH groups of the −1 sugar. A soaking experiment with both acarbose and 4-deoxyglucose resulted in formation of the covalent intermediate, with the +1 site occupied by a 4-deoxyglucose molecule in close proximity to the covalent bond between enzyme and sugar and hydrogen bonded to the Gln-256 side chain. (Figs. 1, *C* and *D*, and 2*B*).

DISCUSSION

Reason for the Formation of the Covalent Intermediate—The observation of a covalent intermediate upon soaking native amylomaltase crystals at pH 5.6 with acarbose was unexpected. Prior structure determinations of covalent intermediates have made use of mutation of the acid/base to impair breakdown of the covalent adduct and of a chemically activated pseudo-substrate like a fluorinated (oligo)saccharide to enable covalent bonding to the nucleophile despite the absence of the acid/base catalyst. In the present case, however, a stable covalent intermediate was obtained without either chemical activation or mutation of any residue. To explain this, the following sequence of events could be imagined. First, acarbose binds in sites −3 to +1, as in the complex structure of Przylas *et al.* (22). Because

[4] T. Kaper, J. C. M. Uitdehaag, T. R. M. Barends, B. W. Dijkstra, M .J. E. C. van der Maarel, and L. Dijkhuizen, manuscript in preparation.

Downloaded from www.jbc.org at University of Groningen on June 28, 2007

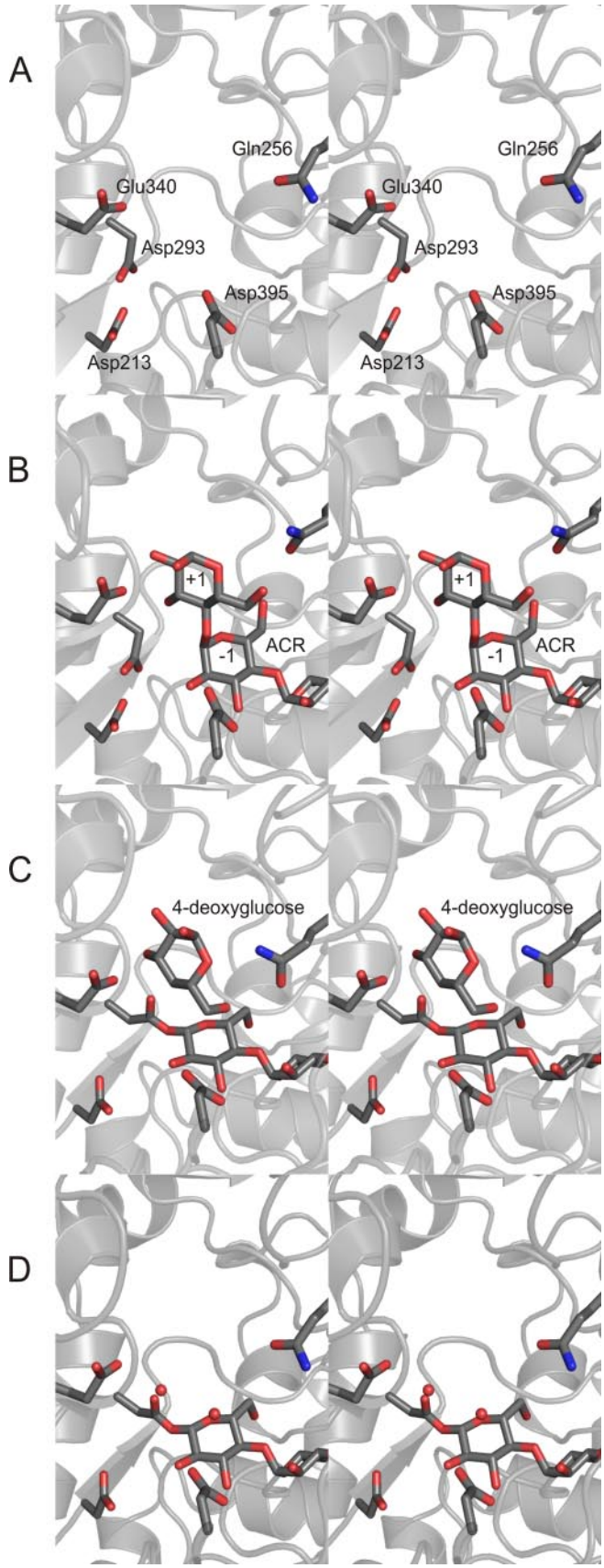

FIGURE 4. **Stereo images of structures representing different states during the reaction cycle of amylomaltase.** *A*, empty active site at pH 5.6. The residues Asp-293, Glu-340, Asp-395, and Gln-256 are indicated. *B*, acarbose (*ACR*) complex as determined by Przylas *et al.* (22). The subsites +1 and −1 are indicated. *C*, acarbose covalent intermediate-4-deoxyglucose complex. *D*, covalent intermediate with acarbose. Possible hydrolytic water molecules are indicated as *spheres*.

the active site residues are all present, the tetrasaccharide is cleaved, leaving a covalent intermediate in sites −3 to −1 while the glucose residue in site +1 diffuses away. To break down this intermediate, only three possibilities exist. First, it could be attacked by a glucose molecule generated by the first half reaction. This is, however, very unlikely, given the volumes and amount of protein that were used; a single protein crystal was soaked in 500 μl of solution, which would lead to a very low concentration of produced glucose (~1 μM). Moreover, the experiment was performed at room temperature, whereas this is an enzyme from a thermophilic organism. This may have slowed down the reaction and contributed to the accumulation of the covalent intermediate.

Second, the intermediate could be attacked by the 4-OH group of another acarbose molecule. Given the acarbose concentration used (~7.5 mM), this may appear more likely but, in fact, is impossible in this crystal form because the hinging movement has brought the 250s loop in a position precluding the binding of a long acceptor beyond subsite +2. The third possibility would be attack by water, but this is very rare in amylomaltases, as will be explained below. Thus, we thank the kinetics of the experiment, the crystal form, and the properties of the enzyme for the unexpected accumulation of the covalent intermediate in the crystals despite a native active site.

Structural Changes during the Reaction Cycle—The available structures allow a detailed view of the changes in conformation of the different reaction partners as they go through the catalytic cycle (Fig. 4). The first structure (Fig. 4*A*) is the empty active site of amylomaltase at pH 5.6. The nucleophilic Asp-293 side chain points away from the active site into the protein where it hydrogen bonds to Asp-213. In this position, the nucleophile is unable to react with the substrate. In contrast, in the *Th. aquaticus* pH 7.5 structure of Przylas *et al.* (23) Asp-293 points into the active site, toward the −1 site, as expected for a catalytically competent conformation, showing that this residue can adopt at least two different conformations.

The next state along the reaction coordinate is the structure of the Michaelis complex with a substrate. Although such a structure has not yet been solved, the acarbose complex structure reported by Przylas *et al.* (22) (Fig. 4*B*) can serve as a model for this state. In this complex, the nucleophilic Asp-293 is in the same catalytically incompetent orientation, hydrogen bonded to Asp-213, as in our pH 5.6 amylomaltase structure. At the time, this was attributed to the high pH of the soaking experiment (pH 9.0), but the pH 5.6 native structure shows that this conformational state can also be populated close to the pH optimum.

Reaction of the enzyme with the substrate leads to the next structure, a covalent intermediate with the leaving group saccharide still in the +1 site, which is represented by the covalent intermediate-4-deoxyglucose complex (Fig. 4*C*). Upon formation of the covalent intermediate, the α-glycosidic bond between the sugar residues in the −1 and +1 sites is replaced by a β-glycosidic bond to Asp-293 via the $O_{\delta 1}$ atom of this residue.

Downloaded from www.jbc.org at University of Groningen on June 28, 2007

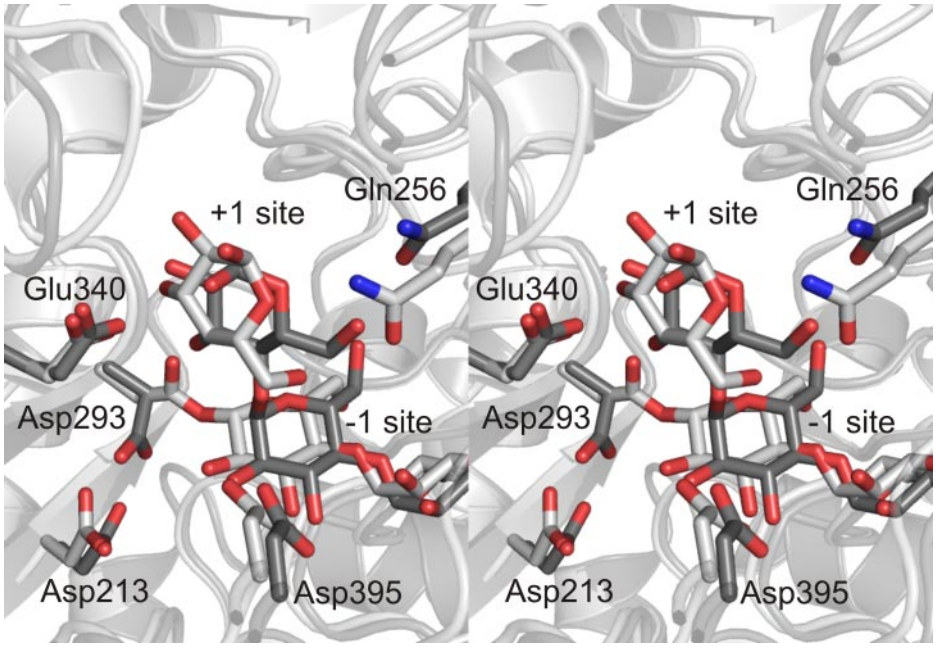

FIGURE 5. **Superimposition of states B and C.** The acarbose complex as determined by Przylas *et al.* (22) in *dark gray* and the covalent intermediate-4-deoxyglucose complex in *light gray*.

To enable formation of this bond from the state in which Asp-293 points into the active site, a rotation around the C_β-C_γ bond has to occur, bringing the C_α-C_β-C_γ-$O_{\delta 1}$ torsion angle from 60° to 168°. From the conformation in which Asp-293 is hydrogen bonded to Asp-213 and points away from the active site a rotation about the C_α-C_β bond would be required as well. Notably, in the covalent intermediate, the plane of the Asp-293 carboxylate group is more or less perpendicular to the plane of the covalently bound −1 sugar (Fig. 4*C*).

A superimposition of the structure of the amylomaltase-acarbose complex (22) with that of the covalent intermediate-4-deoxyglucose complex (Fig. 5) shows that the oligosaccharide in subsite −1 has to move ~1 Å toward Asp-293 to form the covalent intermediate. In the covalent intermediate, the −1 sugar residue has a low energy $^4C_1$ chair conformation (34) as was observed for CGTase (15). Furthermore, compared with the +1 sugar in the acarbose complex the 4-deoxyglucose has rotated by an estimated 20° in the plane of its ring (Fig. 5). However, because the axial C_1-O_1 bond still points in approximately the same direction, this would have few consequences for the continuation of a sugar chain toward the +2 substrate binding subsite and beyond.

This rotation of the +1 sugar seems correlated with the perpendicular conformation of the ester bond with respect to the −1 sugar plane. Without this rotation, the +1 sugar would collide with the Asp-293 $O_{\delta 2}$ (see Fig. 5.). Indeed, the perpendicular orientation of the ester bond seems to shield the anomeric C_1 carbon atom of the covalent intermediate from attack by a nucleophile, both sterically and through charge-charge repulsion, as the $O_{\delta 2}$ has a partially negative charge. Thus, the perpendicular orientation could contribute to the stabilization of the covalent intermediate.

The rotation of the sugar in the +1 site also has consequences for its interaction with the protein, most notably for the interactions with the strictly conserved Gln-256. In the acarbose complex, the +1 sugar contacts Gln-256 only with its O_6 hydroxyl group, whereas in the covalent intermediate-4-deoxyglucose complex both the O_6 and the O_5 are hydrogen bonded to the Gln-256 side chain. Thus, the results show that Gln-256 serves to orient a leaving group (or an incoming acceptor, by microscopic reversibility). Indeed, Kaper *et al.*[4] have found that the Q256N substitution especially decreases the disproportionation activity of amylomaltase with small substrates, which is consistent with a role of Gln-256 in interacting specifically with the +1 monosaccharide.

The next structure is the covalent intermediate structure (Fig. 4*D*) in which the +1 and +2 acceptor sites are empty. In the canonical amylomaltase reaction mechanism, the covalent intermediate would then be attacked by an incoming acceptor molecule through a state as represented by the 4-deoxyglucose-bound structure shown in Fig. 4*C*. As explained above, Gln-256 binds the incoming acceptor, orienting it for attack on the C_1 carbon atom of the covalent intermediate. Possibly, its approach could push Asp-293 out of its "perpendicular" conformation into a conformation with its carboxylate plane more parallel to the −1 sugar ring, perhaps allowing it to bind to the neighboring Arg-291 as in CGTase (15).

Intriguingly, in all of the available structures the acid/base catalyst Glu-340 is hydrogen bonded to the loop containing Asp-293. Thus, as pointed out before, this residue is in a catalytically incompetent conformation as its carboxylate oxygen atoms are >4 Å from the glycosidic oxygen atom that Glu-340 should protonate in the cleavage step (22). It may be that Glu-340 only assumes its catalytic conformation upon binding of an efficacious acceptor, and this may explain why 4-deoxyglucose, which lacks the oxygen that is to be deprotonated in the deglycosylation step, does not trigger the productive conformation of the Glu-340 side chain.

In its incompetent conformation, one of the Glu-340 carboxylate oxygens is at only 3 Å distance from the Asp-293 $O_{\delta 2}$. The proposed conformational change of Asp-293 mentioned above would lead to loss of this interaction, possibly helping Glu-340 to leave its "incompetent" conformation, allowing it to abstract a proton from the 4-OH group of the acceptor. This could be a focal point of further research on glycoside hydrolase 77 enzymes.

Ultimately, all this results in the formation of a new glycosidic bond as in Fig. 4*B*, the acarbose complex. After transglycosylation the newly made sugar chain diffuses away, leaving behind an empty, regenerated active site as in panel A.

Downloaded from www.jbc.org at University of Groningen on June 28, 2007

As an alternative to the formation of a new glycosidic bond, the covalent intermediate may be attacked by a water molecule. However, in the specific case of the *Thermus* enzyme, water is 5000 times less likely to serve as acceptor than maltotriose[4], whereas the covalent intermediates in α-amylases are much more prone to hydrolysis. The covalent intermediate structure presented here provides detailed insight into the cause of the very low hydrolytic activity of amylomaltases. In the canonical mechanism for the hydrolysis of the covalent intermediate in α-amylases, a water molecule activated by the catalytic acid/base attacks the C1 carbon atom of the sugar covalently bound to the nucleophile. In contrast, in amylomaltase, the catalytic acid/base Glu-340 is oriented away from the −1 site such that it is unable to activate a water molecule that could attack the C_1 carbon atom of the covalent intermediate. The unproductive positioning of the catalytic base is thus one obvious explanation for the low hydrolysis rate of amylomaltase.

Conclusions—The amylomaltase structures clarify the role of the conserved Gln-256 as necessary for the correct orientation of an acceptor residue in the +1 subsite. Furthermore, glycosyl transfer in α-amylase-type enzymes benefits from a stabilized covalent intermediate, because this intermediate must be protected from nucleophiles other than the desired acceptor, such as water. The structures presented here show three ways in which amylomaltase stabilizes its covalent intermediate.

First, the covalent intermediate adopts a low energy $^4C_1$ chair conformation, enhancing its stability. This conformation of the covalent intermediate was also observed for the transglycosylases CGTase (15) and amylosucrase (16), but not for the hydrolytic Family 31 α-glycosidase YicI (17). In this latter enzyme, the covalent intermediate has a $^1S_3$ skew boat conformation. This supports the hypothesis put forward by Davies *et al.* (35) and Numao *et al.* (36) that transglycosylases use a low energy $^4C_1$ chair conformation to stabilize their covalent intermediates, whereas in glycosidases the covalent intermediate adopts a more strained conformation, such as a skew boat. Second, the acid/base catalyst is moved out of a productive position in the covalent intermediate structure, precluding it from activating a water molecule, thus protecting the intermediate from hydrolysis.

Finally, third, the plane of the ester bond between nucleophile and sugar is perpendicular to the plane of the sugar ring, which could serve to make the C_1 atom less accessible to an incoming nucleophile because of steric hindrance and charge repulsion by the partially negative $O_{\delta 2}$. These three means of stabilization may also apply to related transglycosylases from glycoside hydrolase families 13, 70, and 77.

REFERENCES

1. Peat, S., Whelan, W. J., and Rees, W. R. (1953) *Nature* **172,** 158–158
2. Peat, S., Whelan, W. J., and Rees, W. R. (1956) *J. Chem. Soc.* **44,** 44–53
3. Palmer, T. N., Ryman, B. E., and Whelan, W. J. (1976) *Eur. J. Biochem.* **69,** 105–115
4. Liebl, W., Feil, R., Gabelsberger, J., Kellermann, J., and Schleifer, K.-H. (1992) *Eur. J. Biochem.* **207,** 81–88
5. Henrissat, B. (1991) *Biochem. J.* **280,** 309–316
6. Henrissat, B., and Bairoch, A. (1996) *Biochem. J.* **316,** 16959–16969
7. Bourne, P. C., and Henrissat, B. (2001) *Curr. Opin. Struct. Biol.* **11,** 593–600
8. Terada, Y., Fujii, K., Takaha, T., and Okada, S. (1999) *Appl. Environ. Microbiol.* **65,** 910–915
9. Takaha, T., Yanase, M., Takata, H., Okada, S., and Smith, S. M. (1996) *J. Biol. Chem.* **271,** 2902–2908
10. Bhuiyan, S. H., Kitaoka, M., and Hayashi, K. (2003) *J. Mol. Catal. B Enz.* **22,** 45–53
11. Strater, N., Przylas, I., Saenger, W., Terada, Y., Fujii, K., and Takaha, T. (2002) *Biologia* (*Bratislava*) **57,** 93–99
12. Kaper, T., van der Maarel, M. J. E. C., Euverink, G. J. W., and Dijkhuizen, L. (2004) *Biochem. Soc. Trans.* **32,** 279–282
13. van der Maarel, M. J. E. C., Capron, I., Euverink, G. J. W., Bos, H. T., Kaper, T., Binnema, D. J., and Steeneken, P. A. M. (2005) *Starch/Stärke* **57,** 465–472
14. Kaper, T., Talik, B., Ettema, T., Bos, H. T., van der Maarel, M. J. E. C., and Dijkhuizen, L. (2005) *Appl. Environ. Microbiol.* **71,** 5098–5106
15. Uitdehaag, J. C., Mosi, R., Kalk, K. H., van der Veen, B. A., Dijkhuizen, L., Withers, S. G., and Dijkstra, B. W. (1999) *Nat. Struct. Biol.* **6,** 432–436
16. Jensen, M. H., Mirza, O., Albenne, C., Remaud-Simeon, M., Monsan, P., Gajhede, M., and Skov, L. K. (2004) *Biochemistry* **43,** 3104–3110
17. Lovering, A. L., Lee, S. S., Kim, Y.-W., Withers, S. G., and Strynadka, N. C. J. (2005) *J. Biol. Chem.* **280,** 2105–2115
18. Svensson, B. (1994) *Plant Mol. Biol.* **25,** 141–157
19. Mosi, R., He, S., Uitdehaag, J. C., Dijkstra, B. W., and Withers, S. G. (1997) *Biochemistry* **36,** 9927–9934
20. Kuriki, T., and Imanaka, T. (1999) *Prog. Biophys. Mol. Biol.* **67,**
21. Davies, G. J., Wilson, K. S., and Henrissat, B. (1997) *Biochem. J.* **321,** 557–559
22. Przylas, I., Terada, Y., Fujii, K., Takaha, T., Saenger, W., and Strater, N. (2000) *Eur. J. Biochem.* **267,** 6903–6913
23. Przylas, I., Tomoo, K., Terada, Y., Takaha, T., Fujii, K., Saenger, W., and Strater, N. (2000) *J. Mol. Biol.* **296,** 873–886
24. Kaper, T., Leemhuis, H., Uitdehaag, J. C., van der Veen, B. A., Dijkstra, B. W., van der Maarel, M. J. E. C., and Dijkhuizen, L. (2007) *Biochemistry* **46,** 5261–5269
25. McPherson, A. (2001) *Protein Sci.* **10,** 418–422
26. Otwinowksi, Z., and Minor, W. (1997) *Methods Enzymol.* **276,** 307–326
27. Collaborative Computational Project Number 4 (1994) *Acta Crystallogr. Sect. D Biol. Crystallogr.* **50,** 760–763
28. Vagin, A., and Teplyakov, A. (1997) *J. Appl. Crystallogr.* **30,** 1022–1025
29. Murshudov, G. N., Vagin, A. A., and Dodson, E. J. (1997) *Acta Crystallogr. Sect. D Biol. Crystallogr.* **53,** 240–255
30. Hayward, S., and Lee, R. A. (2002) *J. Mol. Graph. Model.* **21,** 181–183
31. McRee, D. E. (1999) *J. Struct. Biol.* **125,** 156–165
32. Read, R. J. (1986) *Acta Crystallogr. Sect. A* **42,** 140–149
33. Noguchi, S., Miyawaki, K., and Satow, Y. (1998) *J. Mol. Biol.* **278,** 231–238
34. International Union of Pure and Applied Chemistry (1980) *Pure Appl. Chem.* **53,** 1901–1905
35. Davies, G. J., Ducros, V. M.-A., Varrot, A., and Zechel, D. L. (2003) *Biochem. Soc. Trans.* **31,** 523–527
36. Numao, S., Kuntz, D. A., Withers, S. G., and Rose, D. R. (2003) *J. Biol. Chem.* **278,** 48074–48083
37. DeLano, W. L. (2002) *The PyMol Molecular Graphics System*, Delano Scientific, Palo Alto, CA

Downloaded from www.jbc.org at University of Groningen on June 28, 2007